

AN IMPROVED DATA PROCESSING METHOD FOR CONSOLIDATION COLUMN EXPERIMENTS

Report No. HYD/ET/00/COSINUS8

December 2000

Erik A. TOORMAN & Klaus C. LEURER

A contribution to the MAST III COSINUS project



COSINUSTaskD.1

An improved data processing method for consolidation column experiments

A contribution to Task D.1 of the COSINUS project

REPORT HYD/ET/00/COSINUS8

December 2000

Erik A. Toorman & Klaus C. Leurer

*Hydraulics Laboratory
K.U.Leuven*

Acknowledgements

This work has been carried out within the framework of the MAST3 COSINUS project, funded in part by the European Commission, Directorate General XII for Science, Research & Development under contract no. MAS3-97-0082.

Data from consolidation experiments at T.U. Delft have been made available by Lucas Merckelbach.

The authors post-doctoral position has been financed by the Flemish Fund for Scientific Research (FWO Vlaanderen).

INTRODUCTION

A lasting problem with the accurate prediction of the sedimentation and consolidation behaviour of cohesive sediment is the lack of good constitutive equations for permeability and effective stress. This is partly due to the traditional and conservative geotechnical approach where relationships with void ratio alone are assumed, based on experiments on dense soils under high loading. For self-weight consolidation of soft soils, these relationships are inadequate (Toorman, 1999). Experimental values of both parameters are obtained from data processing of density and pore pressure profiles. Usually, they are plotted against one or the other measure of solids fraction (void ratio, volume fraction, concentration or excess density). These data are then fitted with a simple analytical curve, which is then used as closure. However, it has become clear that neither of these two parameters can be expressed by a unique relationship with solids fraction (e.g. Toorman, 1999).

This report presents a methodology, developed a few years ago by the first author (Toorman, 1996a). The method has been applied at the time to consolidation column test data at the Hydraulics Laboratory of the K.U. Leuven (Toorman, 1996a; Keppers, 1997). However, due to some problems with the measurement equipment, the quality of the data was considered not good enough. Within the framework of the MAST3 COSINUS project new usable data from T.U. Delft has become available. One of these tests has been selected for application of the present data processing method.

EXPERIMENTAL DETERMINATION OF PERMEABILITY

Definition

The permeability k is defined by the (generalized) Darcy-Gersevanov law as the ratio of the settlement rate to the hydraulic gradient (Toorman, 1996b):

$$k = \frac{v_f}{i} \quad (1)$$

where: $v_f = n(v_w - v_s)$ = filtration rate, v_w = averaged water velocity, v_s = settling rate or averaged sediment velocity, $n = 1 - \phi$ = porosity, $i = \partial p_e / \partial z$ = hydraulic gradient, with p_e = excess pore pressure (geotechnical notation). In the case of batch sedimentation (impermeable bottom): $v_f = v_s$.

Pore pressure measurement

The hydraulic gradient is calculated from measured pore water pressure profiles. Pore pressures can be measured with standpipe capillaries or electronic pressure transducers (piezometers). The accuracy of these devices is limited by the instrumentation error and possible problems of air or sediment (partially) obstructing the flow through the filters in the pressure ports.

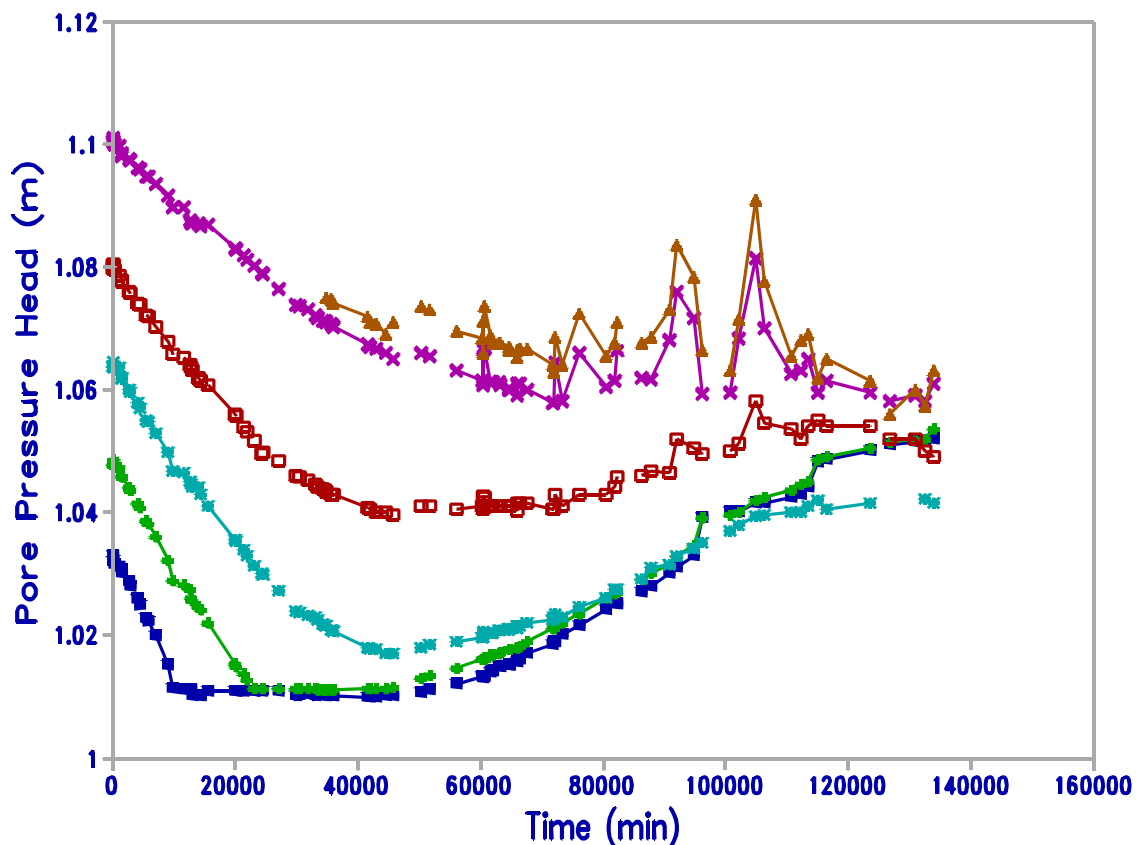


Figure 1: Evolution with time of pore water pressure at various depth of the mud layer in a typical consolidation column test in which fermentation occurs, carried out at the K.U.Leuven (from Toorman, 1996a).

Figure 1 shows the time evolution of the pore pressures measured by six of the eight used standpipes in an older experiment in one of the consolidation columns at the Hydraulics Laboratory of the K.U. Leuven. The curves show initially the dissipation of pore water pressure due to the consolidation process. After ± 5000 minutes pore water pressures rise again due to rising of the water level in the column as the result of gas produced by fermentation. Several aberrant points remain, indicating problems with the pressure ports, but they can be corrected by smoothing the curves.

The highest piezometer (the lowest curve in fig.1) decreases and then suddenly stops when there is no more sediment in suspension above this point. The difference between the piezometer water level and that in the column is the capillary pressure. For simplicity it has always been assumed that the capillary pressure is the same for each of the standpipes, since they are of the same diameter and the same material. However, this need not be the case due to dirt or other disturbances.

Pressure corrections require a high enough recording frequency, such that the time evolution is detailed enough to filter out the erroneous data.

Excess pore pressure calculation

The cheapest and most accurate way to process the pore pressure data to retrieve excess pore pressure profiles is by computing its value relative to the total buoyant stress:

$$\tilde{p}_e = \frac{p_e}{\Delta\sigma_T} = \frac{(p - \Delta p_c) - \rho_w g z - p_o}{\sigma_T - \rho_w g H_o} = \frac{H/H_o - (p - \Delta p_c)/\rho_w g H_o}{1 - \sigma_T/\rho_w g H_o} \quad (2)$$

where: Δp_c = capillary pressure correction, σ_T = total stress at the bottom of the column, i.e. the weight of the water-sediment mixture in the column, $\Delta\sigma_T$ = the corresponding buoyant stress (or submerged weight), $H(t)$ = total column height at time t to include possible water level rise, H_o = initial height of the water column.

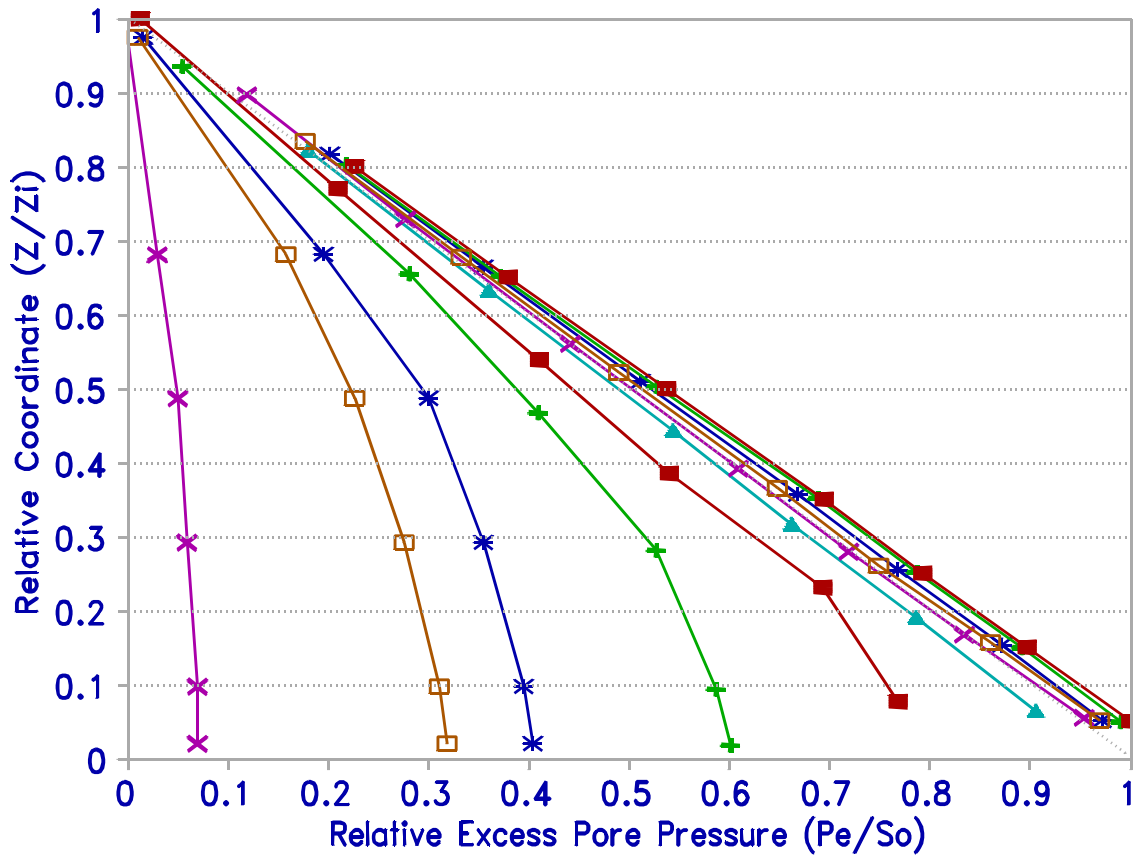


Figure 2: Normalized excess pore pressure profiles for column test Nr.23 after reprocessing (the total buoyant stress seems to have been underestimated) (from Toorman, 1996a).

This formulation only uses the local measured values of pore pressure (and a few precalculated constants). The most orderly presentation is given by the relative excess pore pressures as a function of the relative coordinate $z/z_{interface}$, resulting in the following figure. The excess pore pressure gradient or hydraulic gradient then simply is:

$$i = \frac{1}{\rho_w g} \frac{\partial p_e}{\partial z} = \frac{\Delta \sigma_T}{\rho_w g z_i} \frac{\partial (p_e / \Delta \sigma_T)}{\partial (z/z_i)} \quad (3)$$

and the permeability becomes:

$$k = \frac{v_f}{i} = \frac{v_f}{\frac{\Delta \sigma_T}{\rho_w g z_i} \frac{\partial \tilde{p}_e}{\partial \zeta}} \quad (4)$$

with $\zeta = z/z_i$, the non-dimensionalised level. The big problem is the large error on the experimental excess pore pressures, which is even worse when the gradient must be calculated. Traditionally a simple interpolation of the few experimental points is used. An estimation of the error can be calculated as follows:

- Error on pore pressure measurement: 1 mm water column or 10 Pa, excluding filter malfunctioning (clogging, trapped air) and capillary pressure variations between capillaries.
- Error on column water level: 1 mm water column or 10 Pa (excluding fermentation effects)
- Error on total stress: < 1 % after correction for mass conservation.

Hence, the error on excess pore pressure: > 30 Pa. In practise however, the absolute error is of the order 50-100 Pa.

Proposal for improvement

The fact that the normalized excess pore pressure profiles always seem to show a similar shape trend, created the idea to find an analytical curve fit, which then can be differentiated to obtain a better estimate of the hydraulic gradient. This analytical function must fulfil the following conditions: (1) the gradient at the bottom is always zero; (2) the initial state: $u = y$; and (3) the final state: $u = 0$. At first sight it is not evident to find such a function.

Even though grossly simplified, the analytical solution of *Lee & Sills* (1981) produces normalized excess pore pressure profiles very similar to those obtained in real column tests. The normalized profile is given by:

$$\tilde{u} = \frac{u}{\Delta \rho_s z_o} = 2 \sum_n \frac{(-1)^n \sin(m\pi(1-\zeta))}{m^2 \pi^2} \exp(-m^2 \pi^2 t) \quad (5)$$

with: $m = n + 1/2$ ($n = 0, 1, 2, \dots$), $\zeta = z/z_o$; $T = C_F t/z_o^2$, $C_F = k\phi/\rho_w d\sigma'/de$ (assumed to be constant!).

The excess pore pressure gradient can then be obtained from the y-derivative of eq.(1):

$$\frac{d\tilde{u}}{d\zeta} = 2 \sum_n \frac{(-1)^{n+1} \cos(m\pi(1-\zeta))}{m\pi} \exp(-m^2 \pi^2 t) \quad (6)$$

This method requires the estimation of C_F . Maybe this can be done by first calculating a rough estimate, then try to fit the u -profiles on the experimental ones by adjusting this coefficient.

The plot of the hydraulic gradient profiles, obtained with the Lee & Sills solution, revealed a shape which could be approximated with a much simpler alternative:

$$\frac{d\tilde{u}}{d\zeta} = -\zeta - Y(t)e^{-\zeta/Y(t)} \quad (7)$$

where: $Y(t)$ = a parameter, function of time. Integration yields the excess pore pressure profiles:

$$\tilde{p}_e = 1 - \zeta - Y(t)(e^{-\zeta/Y(t)} - e^{-1/Y(t)}) \quad (8)$$

Comparison of the two solutions (fig.3) reveals that the Lee & Sills solution shows more curvature. The function $Y(t)$ seems to be some sort of power law, as will be shown in the application below. A best fit is found by minimizing the RMS error between experimental data and analytical profile.

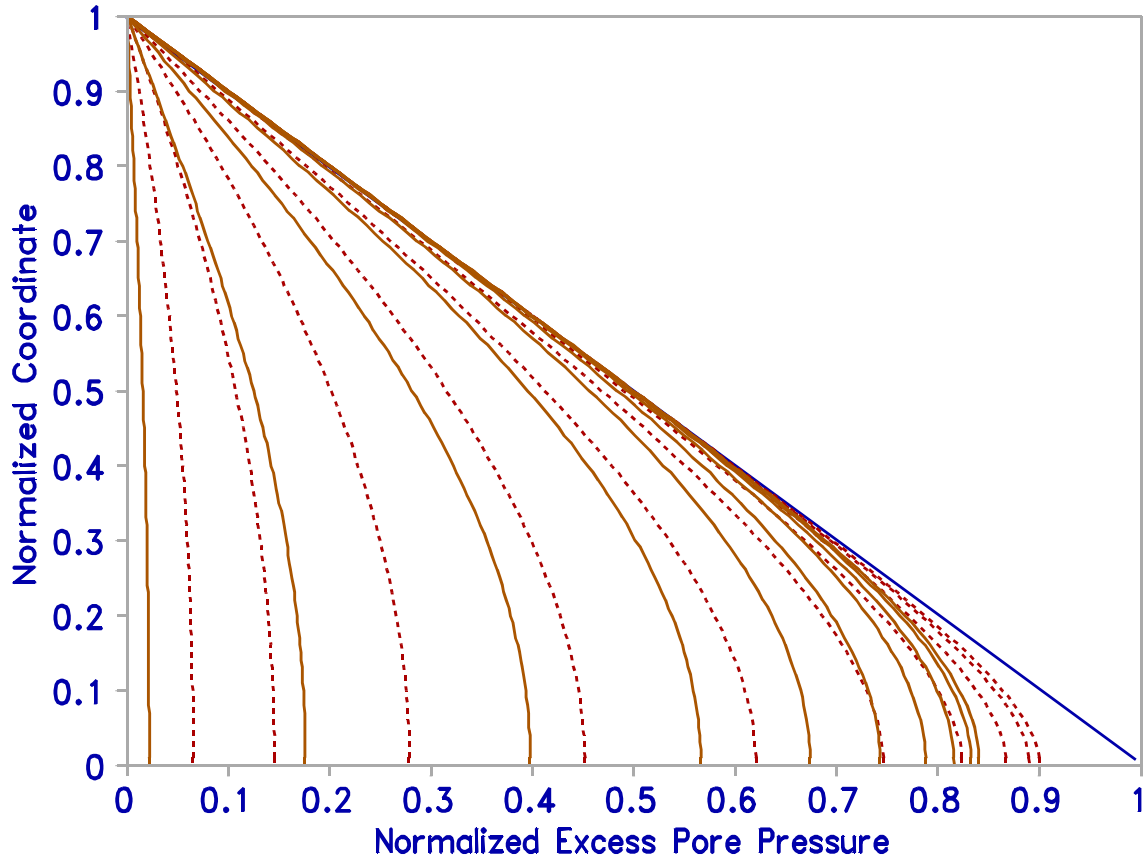


Figure 3: Analytical curve fits for excess pore pressure profiles. Full line = Lee & Sills (1981), eq.(5); dashed lines = present proposal, eq.(8).

The physical background of equations (7) and (8) is not straightforward, except for fulfilling the three basic conditions.

Filtration or Settlement Rate

The settlement rate $w (= v_f)$ can be estimated from the difference between subsequent density profiles in two ways¹:

$$w = \left(\frac{\partial z}{\partial t} \right)_{\text{constant } \sigma} = \left(\frac{1}{g \Delta \rho} \frac{\partial \sigma}{\partial t} \right)_{\text{constant } z} \quad (9)$$

One selects either different levels of constant total buoyant stress ("constant mass points") or take the total stress at the same level for each profile and plot this as a function of time. In both cases large errors are being made by applying a simple first order finite difference discretisation to the time derivative. The error is particularly large because density profile are not frequently enough measured. A second source of error is the inaccuracy of the measurement of the local density.

Up to now a first order forward differentiation is applied, but the hydraulic gradient and density are then averaged over the time interval. Using first order central differentiation does not improve the data (even gives a bit more scatter). Both data overlap and confirm the same trend.

This could be improved by plotting these mass points on the settling curve plot, then connect these points with an analytical curve which should resemble the shape of the interface settling curve. Points out of the expected location (due to the error on the density measurement) could be corrected.

In figure 4 the constant mass points have plotted together with curves obtained from taking the corresponding percentage of the interface level at the same time. In this particular case it seems that the filtration rate then could simply be obtained by taking the fraction of the interface settling rate.

EFFECTIVE STRESS

With the modification of the pore pressure data it is also possible to recalculate the effective stresses. Here, the difference with the traditional method will not be very large.

¹ The second relationship can also be obtained by integration over dz of the mass conservation equation (Gallois, 1995), i.e.:

$$\left(\frac{\partial}{\partial t} \int_0^z \phi dz + [v_f \phi]_0^z \right) \Delta \rho_s g = v_f \Delta \rho g + \frac{\partial(\sigma_{o, \text{total}} - \sigma_o)}{\partial t} = v_f \Delta \rho g - \frac{\partial \sigma_o}{\partial t} = v_f \Delta \rho g - \frac{\partial \sigma}{\partial t} = 0$$

(since $\sigma_{o, \text{total}}$ and p_o do not vary with time).

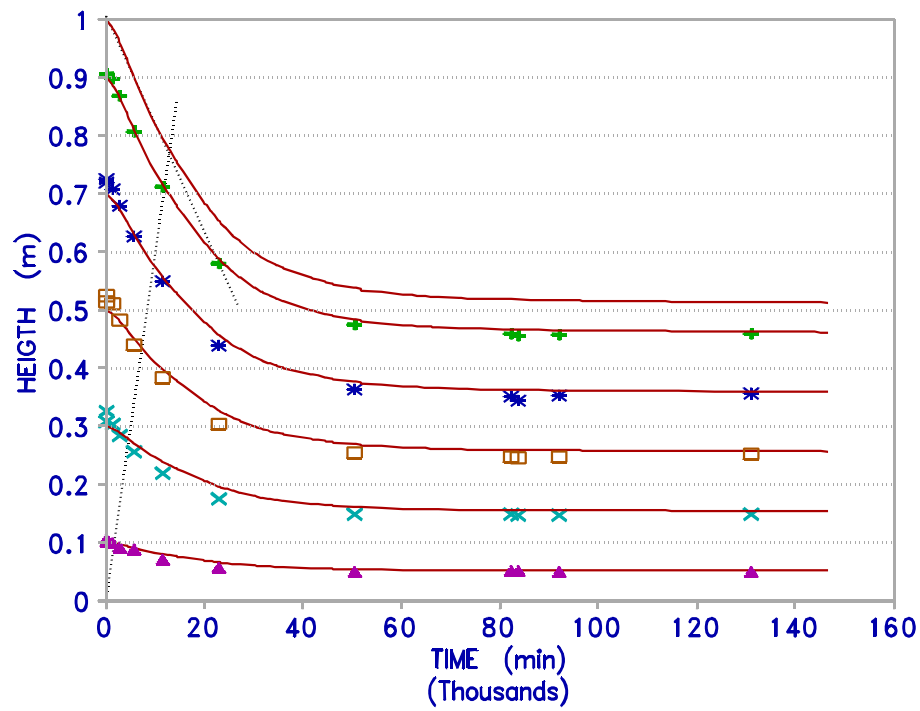


Figure 4: Settling curve (upper line) and constant total stress history data points and corresponding percentual curves (from Toorman, 1996a).

APPLICATION

The new methodology has been applied to the consolidation column test on Dollard mud, carried out at T.U.Delft, within the framework of the COSINUS project (Merckelbach, 1999). Initial conditions were: a homogeneous slurry with density of 1072 kg/m^3 and layer thickness of 1.532 m. Pore pressure were measured at . The solids density was found to be $\rho_s = 2636 \text{ kg/m}^3$. The mud slurry was prepared with tap water with salt added and had a density of $\rho_w = 1003.5 \text{ kg/m}^3$.

Density profiles

The density profiles (figure 5) clearly show that sand has segregated from the slurry in the first stage. The sand forms a layer of approximately 5 cm thickness. The new methodology is only applied to the mud layer above. Therefore, the top of the sand layer is considered as reference level $z = 0$ and the mud layer height or sediment-water interface level is modified accordingly.

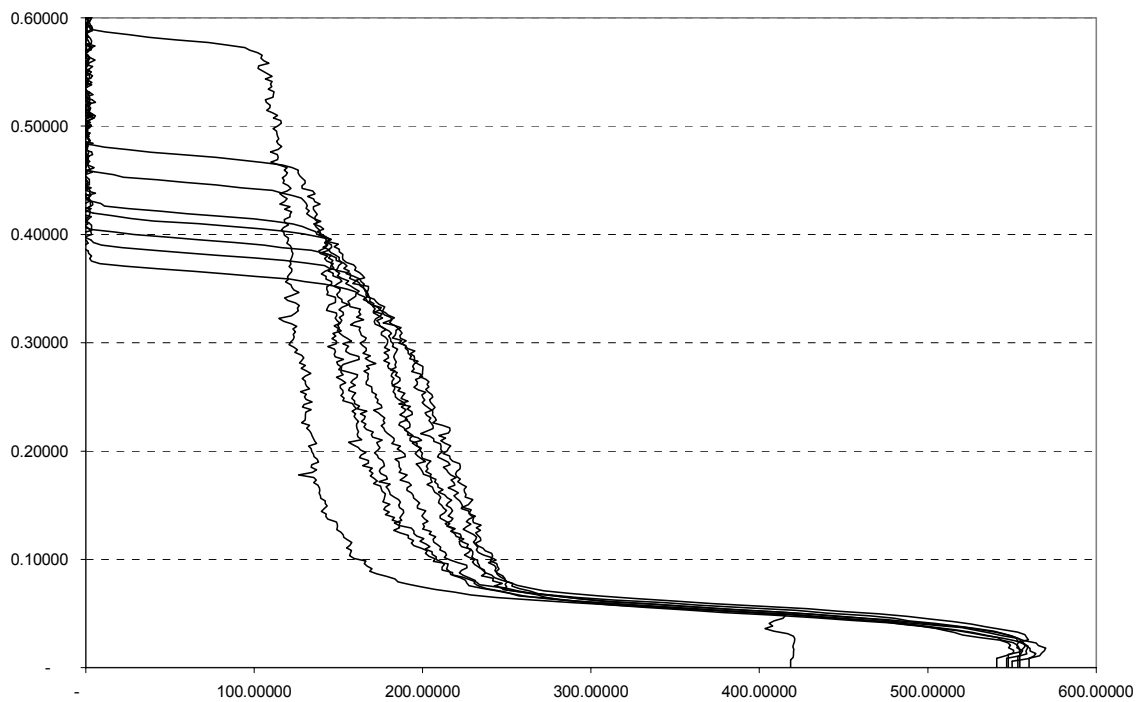


Figure 5: Density profiles at $t = 2, 8, 11, 18, 23, 29, 39, 63$ and 95 days.

Pore pressures

Pore pressures have been measured at heights from 0.5 to 14.5 cm with 2 cm intervals and at 17.5, 20.5 and 30.5 cm from the bottom (Merckelbach, 1998). The normalized profiles are shown in figure 6.

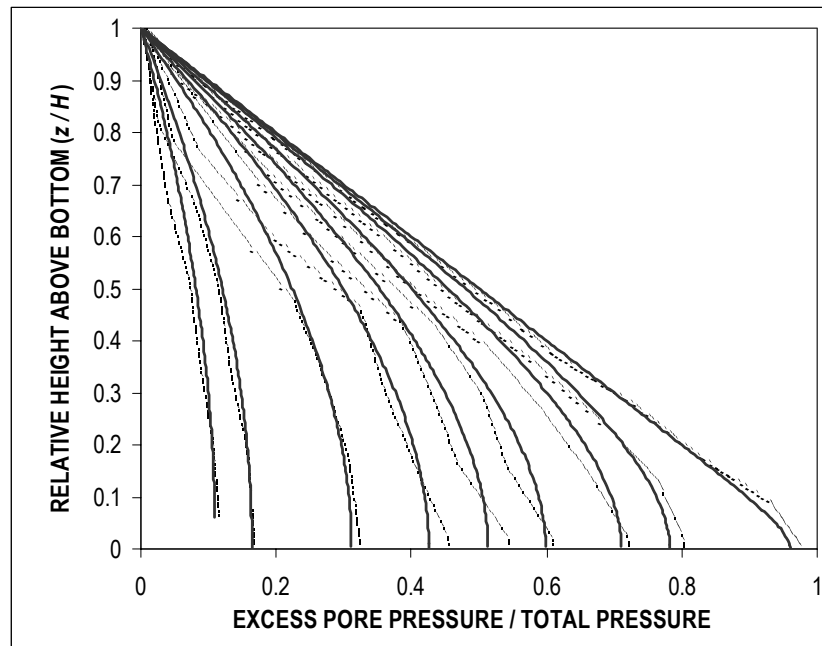


Figure 6: Normalized excess pore pressure profiles for the Dollard mud experiment. Profiles at $t = 2, 8, 11, 18, 23, 29, 39, 63$ and 95 days. Dotted lines = interpolated experimental data, full lines = analytical fit, eq.(8).

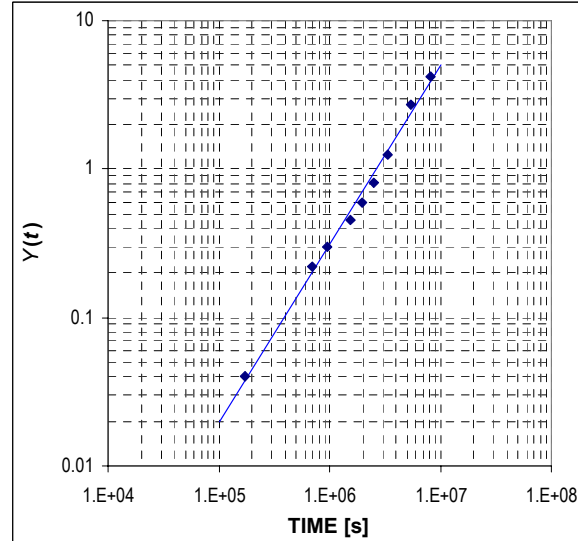


Figure 7: Relationship between the empirical parameter Y and time (t). Symbols = data; line = power law fit, eq.(10).

The excess pore pressure data are fitted with the empirical relationship $Y(t)$, which is given by the power law:

$$Y(t) = A t^n \quad (10)$$

with $A = 2 \times 10^{-8}$ and $n = 1.2$ (figure 7).

Settlement rates

The settlement rates have been determined for layers of constant mass. The mass has been computed by integration from the reference level $z = 0$ using a simple trapezium formula. The data points of the level of the surface of each layers, after the constant settlement period, is plotted against time in figure 4. The data can well be fitted with a simple power law, with nearly the same exponent for each layer (figure 8).

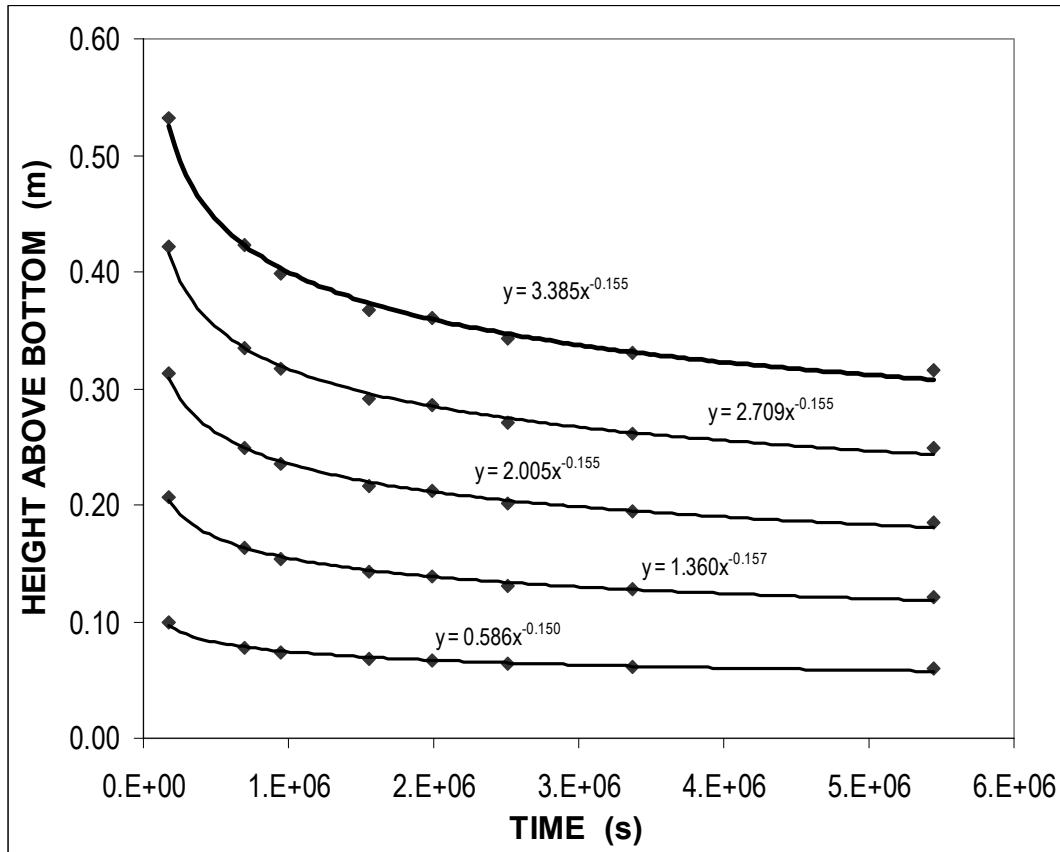


Figure 8: Settlement curves for layers of 20, 40, 50, 80 and 100% mass (from bottom to top). Symbols = data; lines = power law fit.

Also the coefficients of the power law, which have automatically been generated by the *Excell* trendline fitting, show again the proportionality conform the relative mass. These observations imply that the settlement curves show similarity. If this truly is the case, then it should be possible to reconstruct density profiles from knowing the surface settlement and initial conditions alone. This seems to apply only to the primary consolidation where the settlement curve shows a negative power law behaviour and the shape of the density profile is convex ($d^2\rho/dz^2 < 0$). After this stage the density profile becomes concave ($d^2\rho/dz^2 > 0$) and similarity no longer holds.

Permeabilities

The settlement rate is then computed as the derivative with time of the power law. The hydraulic gradient is computed with eq.(7). Hence, the permeabilities are obtained. The results (figure 9) show significantly less scatter than the permeabilities obtained according to the traditional methodology (compare figures 10 top and bottom).

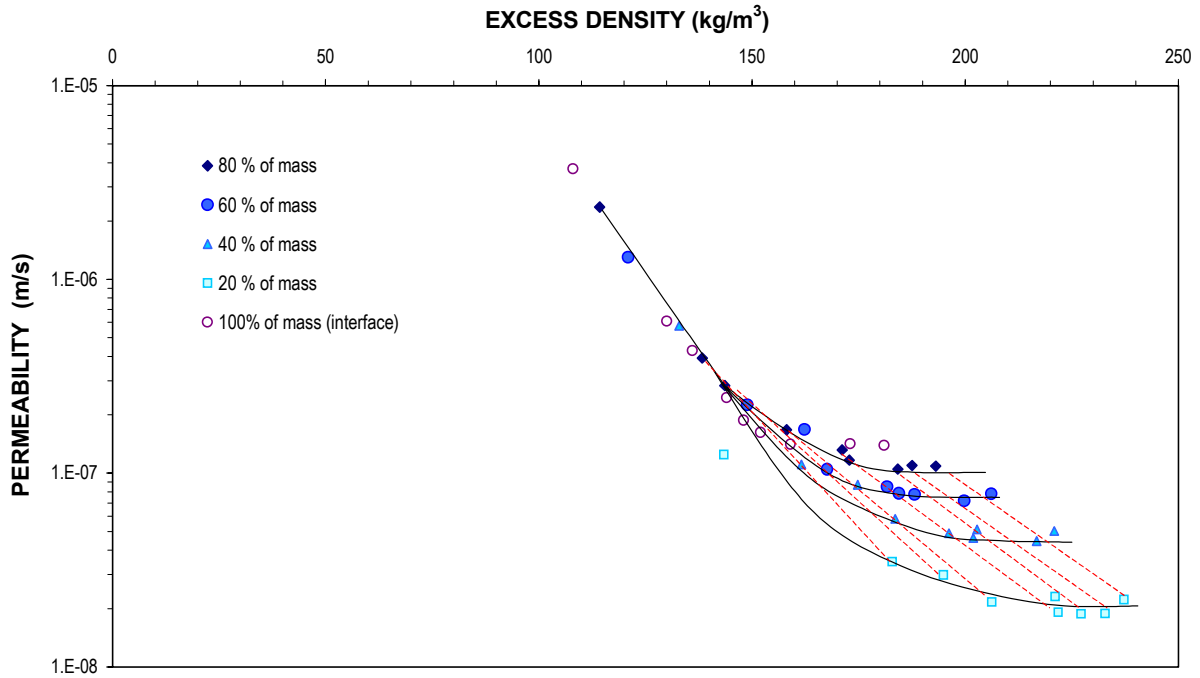


Figure 9: Evolution of permeabilities of 5 layers of the mud bed. Dashed lines connect points corresponding the same moment.

The results show distinct differences in the permeability-density relationship for each layer, i.e. showing lower permeabilities for the same density with increasing depth. This implies that the permeability decreases with increasing effective stress, i.e. the submerged weight of the sediment above.

Permeabilities for the mud layer at the same time are connected with the dashed lines, moving from left to right with increasing time. They seem to indicate that the instantaneous slope of $\log(k)$ versus excess density slowly increases.

The permeability tends to remain constant with increasing density when approaching the end of primary consolidation (i.e. total dissipation of excess pore pressures). As this phenomenon occurs in each layer, the curvature in the k - Δp relationships cannot be attributed to the influence of segregated sand. The sand layer, which has been excluded from the above analysis, gives very different k values, as can be seen in figure 10 (top), obtained by Merkelbach using a traditional method.

Both observations imply that the structure of the bed changes. The most likely explanation is that the lower-order aggregates, which are strong enough not to break up under the load (effective stress), rearrange, such that open pores along which drainage occurs reduce

in size. Near the surface, it is expected that more pore water can be captured within pore spaces, which block certain drainage path ways.

A conceptual mathematical approach can be made in order to verify this hypothesis. Approximating a mud layer surface by a continuous array of pipes, for which Poiseuille flow is assumed, yields a permeability of:

$$k = \frac{\rho_w g r^2}{6 \mu_w} (1 - \phi_e) \quad (11)$$

where: r = the average radius of the (open) pores, ϕ_e = the effective un-available space, i.e. the volume fraction of the sediment and of the immobilized pore water. Considering a density of 1200 kg/m^3 , i.e. $\phi_s = 0.12$. At the surface, it is assumed that the bed structure can be compared to a maximum packing at $\phi_e = 0.65$ of aggregates which can hold their pore water. With increasing depth, and thus effective stress, the value of ϕ_e will decrease, but cannot become smaller than ϕ_s . In order to obtain a decrease in permeability with depth, r^2 should decrease faster than that $1 - \phi_e$ increases. For the extreme case of ϕ_e decreasing from its maximum to its minimum value, r should decrease at least by a factor of only 1.6, which is much lower than what is expected to happen in reality. Hence, a decrease of k with depth for the same density can be explained in this way.

The interface data deviate most from the other layers, but this can be attributed to underestimation of the true surface density and the difficulty of determining the exact level of the interface (uncertainty of the order $\pm 1 \text{ cm}$). Nevertheless, the same trend can be seen as in the other layers.

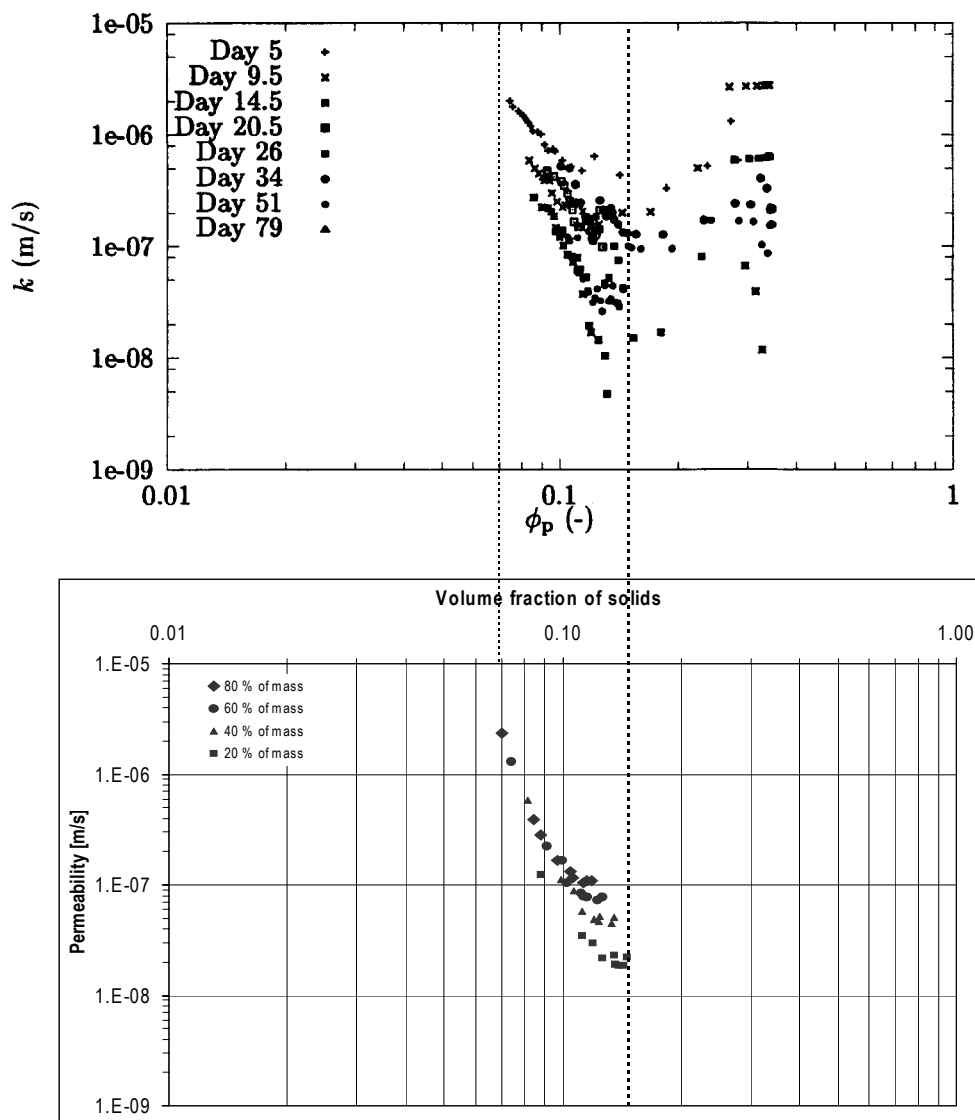


Figure 10: Comparison between permeabilities computed according to the traditional (top, figure A.21 from Merckelbach, 1999) and the new methodology (bottom). Only the range between dotted lines should be compared (data points for high solids fractions in the top figure corresponds to the sand layer).

REFERENCES

- Gallois, S.** (1995). Modélisation de la sédimentation-consolidation et expérimentations sur les vases estuariennes. PhD thesis, Université de Nantes.
- Keppers, C.** (1997). Improved data processing for consolidation tests. Ind. Engr. thesis, Katholieke Hogeschool St.-Lieven, Gent (in Dutch).
- Lee, K. & G.C. Sills** (1981). The consolidation of a soil stratum, including self-weight effects and large strains. *Int. J. Numerical and Analytical Methods in Geomechanics*, Vol.5:405-428.
- Merckelbach, L.M.** (1998). Laboratory experiments on consolidation and strength evolution of mud layers. Report TUD 1-98, Hydromechanics Group, Faculty of Civil Engineering and Geosciences, Technical University Delft, 67 pp.
- Merckelbach, L.M.** (1999). Consolidation and strength evolution of Dollard mud. Measurement report on laboratory experiments. Report TUD 4-99, Hydromechanics Group, Faculty of Civil Engineering and Geosciences, Technical University Delft, 48 pp.
- Toorman, E.A.** (1996a). Some ideas for improving data processing of settling / consolidation column experiments. Internal Draft Report, Hydraulics Laboratory, Katholieke Universiteit Leuven.
- Toorman, E.A.** (1996b). Sedimentation and self-weight consolidation: general unifying theory. *Géotechnique*, Vol.46(1):103-113.
- Toorman, E.A.** (1999). Sedimentation and self-weight consolidation: constitutive equations and numerical modelling. *Géotechnique*, Vol.49 (No.6):709-726.